Power Plant Control in Large Scale PV Plants. Design, implementation and validation in a 9.4 MW PV plant

***Eduard Bullich-Massagué*[1], *Ricard Ferrer-San-José*[1], *Mònica Aragüés-Peñalba*[1], *Luis Serrano-Salamanca*[2], *Carlos Pacheco-Navas*[2], *Oriol Gomis-Bellmunt*[1]**

[1] *CITCEA-UPC, Electrical Engineering Department, Technical University of Catalonia, Diagonal 647 Planta 2, Barcelona, Spain*
[2] *GreenPowerMonitor, Avda. Josep Tarradellas 123-127, 08029 Barcelona, Spain*

Keywords: PV plant, control, modelling, simulation, grid code

Abstract

The paper proposes an algorithm for active and reactive power management in large PV power plants. The algorithm is designed in order to fulfil the requirements of the most demanding grid codes and combines the utilisation of the PV inverters, fixed switched capacitors and STATCOMs. The control algorithm is simulated as required by the grid codes and validated on a real 9.4 MW photovoltaic power plant.

1 Introduction

With the electric energy demand increasing and the rising awareness around sustainable growth (e.g. the well-known 20/20/20 objective [1]), renewable energies have experienced a rapid growth in the last few years [2, 3]. In the electricity sector, wind power and photovoltaic (PV) power are the technologies with the highest growth in Europe [4]. Currently, the amount of energy generated from PV or wind power has a great importance in the energy mix. With the increase of renewable penetration, the grid support provided by these sources is fundamental. As a result, new grid codes are appearing or being updated, forcing wind and PV power plants to provide grid support [5–10]. The most demanding grid codes are normally those of island areas or weak power systems.

Power management applied to PV plants has encountered many technical challenges. For instance, the integration of storage systems to deal with the variability of the renewable sources and the appropriate coordination with the power plant control, which has been addressed in [11–19]. The authors from [11] propose a control method for a battery energy storage system to be integrated in renewable plants so that the intermittent resource can be dispatched on an hourly basis. In [12], a power plant control for a PV plant is proposed to accomplish grid code requirements, comparing the operation when the PV plant includes storage support and when it does not. Focusing on the ramp rate control, a model to simulate effective dispatch of energy storage units so as to ensure this requirement is shown in [13]. A different approach for PV inverter ramp rate control, also using an integrated energy storage device, is suggested in [14]. It is proposed as a more accurate solution than the traditional moving average method, for allowing to limit the ramp-rate within a desired level. The utilization of PV solar farm inverters as STATCOMs for improving power transfer limits is addressed in [20]. The Low Voltage Ride Through requirement is examined in [21], proposing a control strategy to improve voltage profiles in steady state and when facing load variations at grid buses [16]. The authors from [18] propose a control coordination for capacitor banks and an on-load tap changer in a wind power plant to accomplish the grid code requirements. This proposal is based on the knowledge of the capacitor's state by the central controller, thus bidirectional communications are required. On the other hand, in [19] an algorithm for the coordinated control of automated devices and photovoltaic generators is presented, based on an optimization approach for minimizing circuit losses and motion of utility controls while solving voltage rise problems. However, the analysis does not take into account the controls needed and their dynamics.
The before cited studies analyse specific devices and/or strategies that can enhance the grid integration of PV plants by affecting the power management. A global approach on the active and reactive power controls needed to fulfil the grid codes requirements and their interaction is addressed in this paper, which extends the basic concepts presented in [17]. The control proposed does not need to know the power production state of each converter and the communication system needed is unidirectional. Furthermore, the experience in the PV plant commissioning process is shown and real tests results are presented to validate the algorithms proposed.

Figure 1 shows the sequence followed to manage the PV plant project development in different countries as Romania, South Africa or the U.S.A. Grid code requirements have implications in PV plant design and control. Most of the plants to be controlled have already been constructed, so the focus is to design a control and, if needed, to redesign the PV plant adding, for instance, FACTS devices. After addressing the control algorithms, transmission system operators (TSO) require simulation models of the PV plants including their control. So, the corresponding models are made in PSS/E® and DIgSILENT Power Factory® software, as it is indicated in most grid codes [6–8]. After performing some simulations and validating the grid code compliance, the implementation is permitted and own tests are made before the TSO performs the validation tests to consider the PV plant able to be operative. Due to different PV plants studied, a general control model is designed using the typical ancillary devices such as FACTS and capacitor banks.

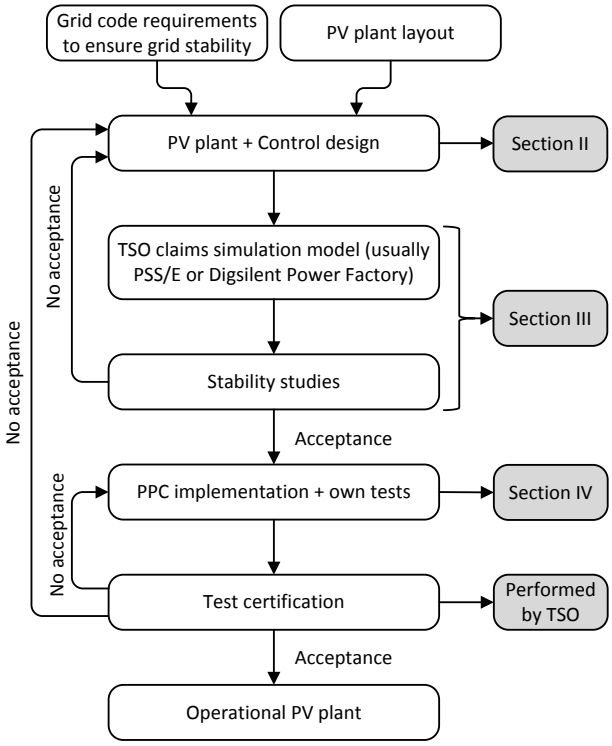

Fig. 1: PV plant control design and implementation process

2 Power Plant Control Design

2.1 PV Plant Description

Although there is no clear categorization on PV plants size according to the installed capacity, the ones considered in this study could be classified as large scale PV plants for presenting an installed capacity of 9.4 MW, which is in the range from several MW to GW, considered large scale [22]. As shown in Figure 2, each PV inverter is associated to a PV string and connected to a three winding transformer. This transformer elevates the voltage from low to medium voltage and is connected to an internal PV collection grid (usually in tree or ring configuration). Ancillary devices as FACTS or capacitor banks are connected to the internal PV grid or to a collector bus close to the MV/HV transformer. The MV/HV transformer connects the PV collection grid to the high voltage transmission system.

Despite having local controls, it is necessary to coordinate PV inverters together to achieve the desired setpoints at the point of common coupling (PCC). Hence, a power plant control (PPC) must act as a master to drive all PV plant devices. In this way, the PPC will read the measurements from the PCC and will send orders (active and reactive power setpoints) to all inverters or FACTS, as well as connection/disconnection orders to capacitor banks if they are present in the PV plant. Then, the inverters will perform their own controls to follow their master (PPC) orders. Only in the case of fault ride through (FRT), inverters and FACTS will omit the PPC orders. This is due to the fact that grid codes require a rapid response during fault events where a communication delay would result in the PV plant being non-compliant to the FRT requirement.

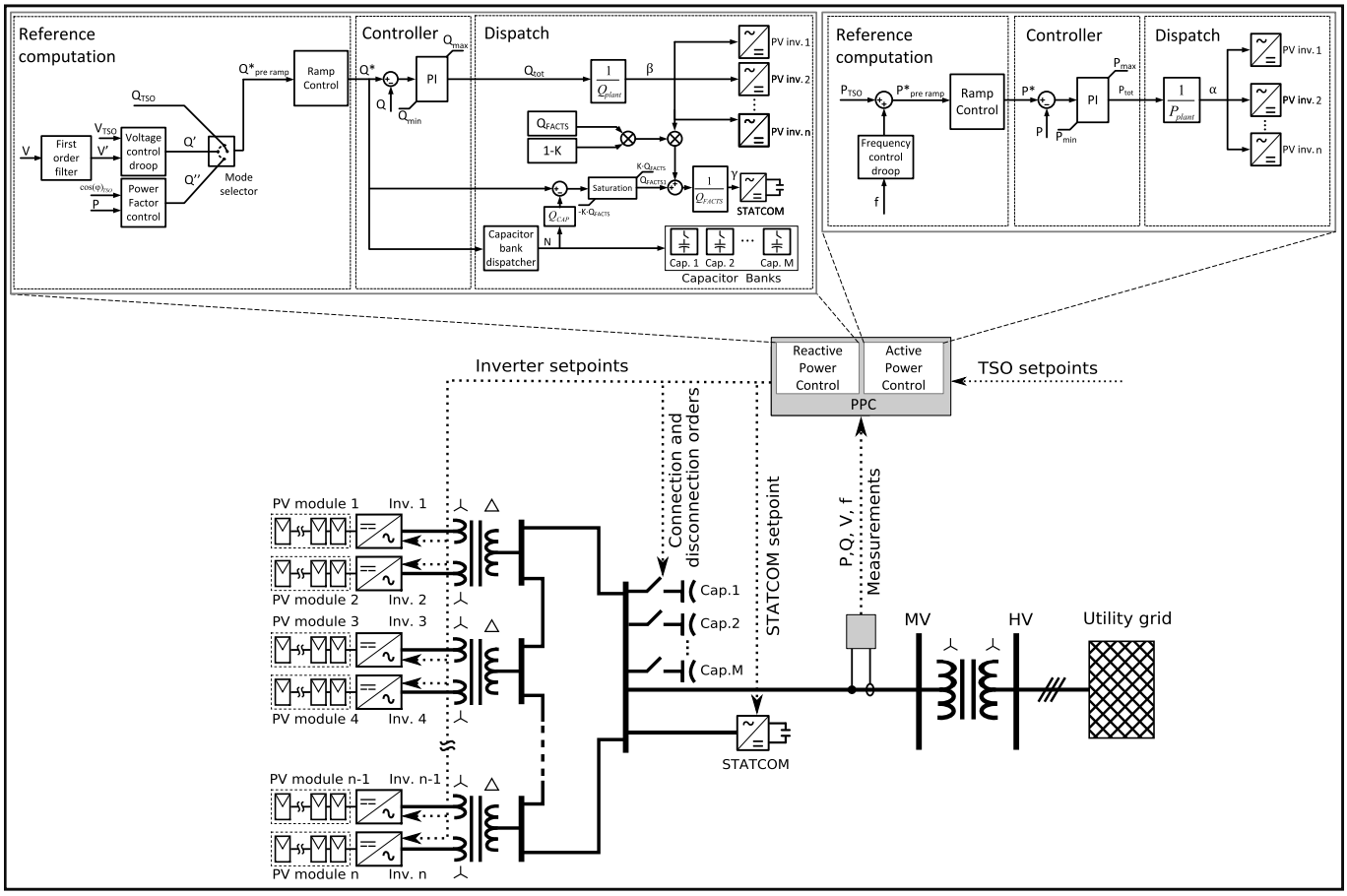

Fig. 2: Typical large scale PV plant layout including the proposed power plant control schemes

2.2 Control Requirements

Grid code requirements [5–10] can be summarized in i) voltage regulation actions, ii) frequency regulation actions, iii) FRT actions and iv) ramp rate restrictions:

i) Voltage regulation actions: the PV power plant is required to help maintaining the grid voltage level. A minimum reactive power capability of the PV power plant is established. Additional ancillary equipment, as FACTS devices, can help to reach the capability limits. Depending on the TSO needs, the actions required in voltage regulation can be chosen from:

- Reactive power setpoint: the TSO sends a reactive power setpoint that must be exchanged at the PCC.
- Voltage regulation by droop curve: the TSO specifies a droop curve which consists of predefining the reactive power depending on the voltage level at the PCC.
- Power factor setpoint: the TSO sends a power factor setpoint to be established at the PCC.

ii) Frequency regulation actions: the frequency support is required to maintain the grid frequency between specified ranges around its nominal value. The frequency support may require, depending on the country, some kind of energy storage system [8]. The basic requirements in this field may be summarized as:

- Active power curtailment: the TSO sends an active power setpoint to be injected at the PCC.
- Frequency regulation by droop curve: The TSO specifies a curve which predefines an increase or decrease of the active power delivered at PCC as a function of the measured frequency.

  In absence of power reserve provided by energy storage system or auxiliary generation system (e.g. diesel generator), the increase of power generation when the plant is operating at its maximum power point (MPP) cannot be done. So, agreements

with TSO are performed and in these conditions (MPP operation and absence of reserve) underfrequency droop curve is not applied. Note that the frequency droop function is also required to be applied during curtailment events. In this case, underfrequency support can be performed.

iii) FRT actions: the fault support specifies requirements under abnormal conditions at PCC. The main specifications in this field are a dynamic reactive power injection requirement under fault conditions, and the time that the power plant must remain connected to the grid depending on the voltage and frequency levels reached during the fault.

iv) Ramp rate restrictions: The active power variation may be restricted to a ramp rate when transitions (like curtailment setpoint) occur if the plant does not include energy storage systems [6, 7]. When a power plant is provided with energy storage systems as required in [8], it is possible to limit the power output variation at any time. Ramp rates also may be applied to reactive power output [7].

2.3 Power Plant Control Solution

Taking into account that PV inverters have the capability to perform their own local controls following active and reactive power setpoints, the PPC will generate these setpoints in order to achieve the desired value at PCC. PV inverters including their local control are already built. So, only the PPC, which drives the voltage and frequency support actions listed above is described here. The FRT requirement is fulfilled by the local controls.

The active power control scheme is shown in Figure 2. The control is divided in the reference computation block, the controller and the dispatch system.

The reference computation block calculates the active power setpoint that must be achieved at PCC. Despite the TSO may send a curtailment setpoint, P_{TSO}, a frequency droop is applied continuously so that it modifies the desired setpoint at PPC, $P^*_{pre-ramp}$. Furthermore, there is a ramp rate limitation provided by the grid code. So, $P^*_{pre-ramp}$ is limited by a ramp rate controller which computes the desired active power at the PCC, P^*.

If there is not a curtailment event, P_{TSO} is set to the nominal PV plant power, P_{plant}. The frequency droop curve is set in the most generic shape which corresponds to that described in [6] and shown in Figure 3(a), where $P_{available}$ is the maximum available active power, P_{TSO} is the TSO curtailment setpoint, P_{min} is the active power that the PV plant has to deliver when a maximum overfrequency deviation, f_{max}, occurs (for frequencies over f_{max} it is permitted to disconnect), f_4 establishes when the overfrequency droop finishes and P_{min} must be delivered, f_n is the nominal frequency (the TSO can modify it sightly according to its necessities), f_2 and f_3 determine a deadband zone where the frequency droop is not applied, f_1 establishes when the underfrequency droop finishes and f_{min} is the maximum underfrequency deviation where the PV plant must remain connected. The definition of the frequency droop curve is done according to [6], where TSOs specify the *dead band*, f_{min}, P_{min}, f_{max}, *Droop 1* and *Droop 2*. As mentioned before, agreements with TSOs are made to implement the frequency droop curve in absence of power reserves. In the case of the PV plant operating at the MPP (no curtailment required), $P = P_{available} \leqslant P_{TSO} = P_{plant}$. Under this condition, P_{TSO} is greater than $P_{available}$ and the TSOs have agreed to implement the curve depicted in Figure 3(b). In this situation, once the frequency exceeds the threshold, f_3, P_{TSO} is fixed at the current active power value and the over frequency droop operation is performed. During curtailment events, $P_{TSO} < P_{available}$ and the curve of Figure 3(a) is implemented.

Once P^* is obtained, the controller computes the aggregated power, P_{tot}, that must be generated by all PV inverters. The controller is based on a typical PI controller which ensures the error between P^* and the measured power at PCC, P, to be 0 in a steady state.

The dispatch system is applied using p.u. signals as in [23]. However, the present approach does not need any information of the available power.

The dispatch system takes the P_{tot} and distributes it among all PV inverters. It is dispatched in a per unit system so that there is only 1 signal to be sent despite different PV inverter power ratings. In this way, P_{tot} is divided by the nominal PV plant power, P_{plant}, to obtain α that is sent to all inverters. Each inverter *i* receives the α signal and computes its local active power setpoint according to the expression (1).

$$P^*_{inv,i} = \alpha \cdot P_{nom,i} \tag{1}$$

Where $P_{nom,i}$ and $P^*_{inv,i}$ are the nominal active power and the local active power setpoint of the inverter *i* respectively.

The reactive power control is performed similarly to the active power control. Figure 2 depicts its corresponding scheme. In addition to PV inverters, FACTS devices or capacitor banks are commonly found in a PV plant. So, the control is designed for a

generic PV plant which can contain all these elements. To do so, a priority criteria has been established. First, capacitor banks are managed to deliver the major part of reactive power (only when capacitive power is required). These banks deliver discrete blocks of reactive power so, the fine regulation is performed by FACTS and PV inverters. FACTS have priority over PV inverters as they are installed for this particular application. However, when a FACTS device reaches a specified level of reactive power (not necessarily its nominal power) the remaining amount of reactive power is delivered by both (FACTS and PV inverters).

Contrary to the frequency regulation actions, the voltage regulation actions do not require simultaneous operations as for example reactive power setpoint plus voltage droop. So, a mode selector is implemented to determine the way to calculate the desired reactive power setpoint, $Q^*_{pre-ramp}$. If the TSO sends a reactive power setpoint, Q_{TSO}, then $Q^*_{pre-ramp} = Q_{TSO}$. When power factor setpoint is set, the corresponding desired reactive power is calculated as (2). When a voltage droop mode is set, the $Q^*_{pre-ramp}$ is calculated according to a curve depicted in Figure 3(c). In this case, due to the whole plant operation, it is needed to filter the voltage measurement, V, to obtain the droop input, V'. This filtering is to avoid multiple connections/disconnections of the capacitor banks (a connection of a capacitor bank provokes a voltage increase and so, a decrease of $Q^{'}$ and the corresponding capacitor disconnection). With this filter and an hysteresis applied to capacitor bank dispatcher, the multiple connections/disconnections are avoided. When there are not capacitor banks, the time constant of the filter is set to 0.

$$Q^*_{pre-ramp} = P \cdot \frac{\sin(\varphi)_{TSO}}{\cos(\varphi)_{TSO}} \tag{2}$$

Where P is the measured active power at PCC and $\cos(\varphi)_{TSO}$ is the power factor setpoint.

Once $Q^*_{pre-ramp}$ is obtained, it can be limited (or not, depending on the grid code) by a ramp rate limiter obtaining the desired reactive power at PCC, Q^*. At this point, if Q^* is capacitive, capacitor banks (if they are available) generate the major part of Q^*. This is performed by taking the setpoint and calculating the number of capacitors to be connected in the capacitor bank dispatcher. The connection orders of capacitor banks are set according to the following criterion (3) and (4) and are represented in Figure 4.

Connection/disconnection orders for the i-th capacitor bank:

$$\text{SET}_{CAP_i} = Q^* > (i - 0.4) \cdot Q_{CAP} \tag{3}$$

$$\text{RESET}_{CAP_i} = Q^* < (i - 0.6) \cdot Q_{CAP} \tag{4}$$

Where Q_{CAP} is the reactive power supplied by a capacitor bank at nominal voltage.

Then, the finer control is performed first by FACTS and with PV inverters afterwards. A factor $K \in [0, 1]$ determines the amount of reactive power that is supplied only by FACTS devices. In a first stage, Q_{FACTS1} is calculated according to (5) with a maximum absolute value of $K \cdot Q_{FACTS}$, where Q_{FACTS} is the nominal reactive power of the FACTS device.

$$Q_{FACTS1} = Q^* - N \cdot Q_{CAP} \tag{5}$$

Where N is the number of capacitor banks connected.

Then, the controller computes the rest of the reactive power that FACTS plus PV inverters have to supply, Q_{tot}. It is performed by a PI controller as shown in Figure 2, and the corresponding p.u. value β is calculated by dividing Q_{tot} by Q_{plant}, where Q_{plant} is the nominal reactive power of the PV plant. At this point, as the available reactive power remaining in the FACTS device is $(1 - K) \cdot Q_{FACTS}$, the additional part of FACTS contribution is calculated as $\beta \cdot (1 - K) \cdot Q_{FACTS}$. The total reactive power setpoint to the FACTS device in a per unit system is calculated as (6).

$$\gamma = \frac{Q_{FACTS1} + Q_{FACTS} \cdot \beta \cdot (1 - K)}{Q_{FACTS}} \tag{6}$$

Each PV inverter *i* receives the β signal and computes its local reactive power setpoint according to the expression (7).

$$Q^*_{inv,i} = \beta \cdot Q_{nom,i} \tag{7}$$

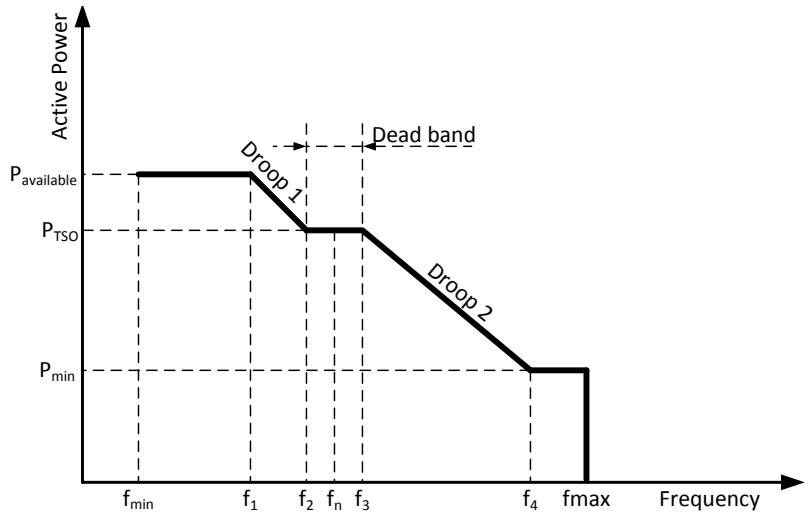

(a) Generic frequency droop curve

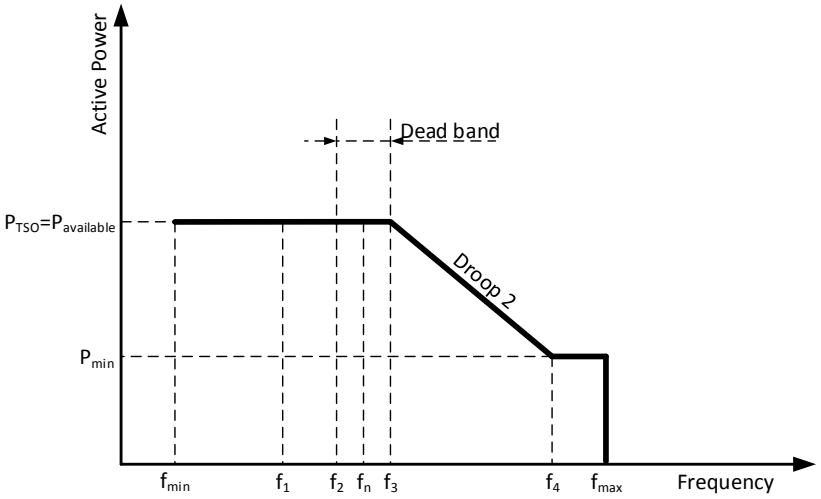

(b) Frequency droop curve in absence of curtailment event

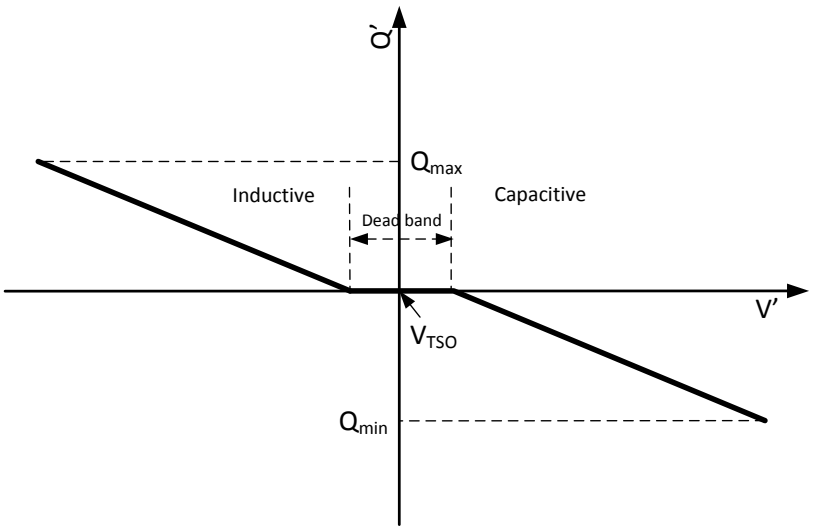

(c) Voltage droop curve

Fig. 3: Droop curves for frequency and voltage regulation

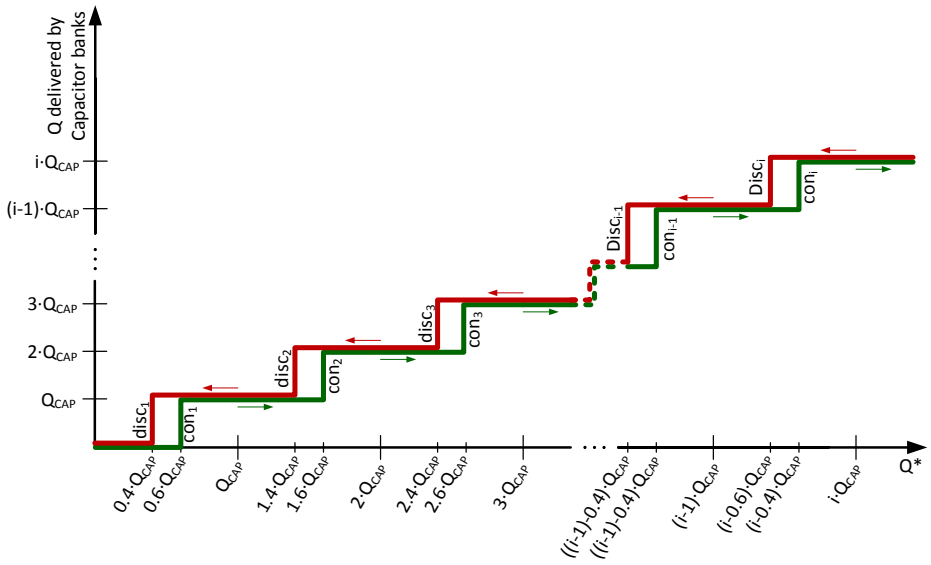

Fig. 4: Capacitor bank connection/disconnection criterion

Where $Q_{nom,i}$ and $Q^*_{inv,i}$ are the nominal reactive power and the local reactive power setpoint of the inverter *i* respectively.

The FACTS device receives the γ signal and computes its local setpoint according to (8).

$$Q^*_{FACTS} = \gamma \cdot Q_{FACTS} \tag{8}$$

Where Q_{FACTS} and Q^*_{FACTS} are the nominal reactive power and the local reactive power setpoint of the FACTS device.

Remark: for under frequency events, the PV plant will tend to operate at its MPP, while for over frequency operation, the plant will not run at its full capacity and PV power will be wasted. Despite this drawback, the system stability must be ensured. When large amount of PV or any intermittent power generation is (and will be) connected to the grid, this stability will not only depend on the conventional generation response but also on the operation of these renewable power plants. A waste of PV power will be a requirement to maintain the grid frequency between the limits and hence, the power quality during these events, except if there are energy storage systems capable of shifting the power generation. The energy storage systems are still expensive and most of them under development, demonstration or early commercialized [24].

3 Modelling and Simulation

All controls explained above have been modelled in a way that they can be treated as a black box where the user (TSO) can connect the required measurements and the outputs (α, β, γ and capacitor banks orders) to the required devices. Most of the parameters detailed in section III are configurable: droop curves, PI controller parameters K_P, K_i and K_w (antiwindup constant), ramp rate limits, sample times, communication delays, etc.

3.1 PV Plant Modelling Aspects

The active and reactive power management algorithm model has been created in FORTRAN language for PSS/E® software where corresponding simulations are performed in RMS values. The need to use this software comes from the grid operator that includes it into the corresponding grid code.

The PV plant model corresponds to the Vanju-Mare PV plant (Figure 5). The PV plant is located in Romania close to the village of Bucara covering a total area of 23.4 ha ($234 \cdot 10^3$ m^2) [25]. It consists of 15 PV inverters with a total peak power of 9.4 MW [26]. The PV inverters are connected to a 20 kV PV collection grid in ring configuration and then, to a 110 kV transmission grid through a MV/HV transformer. Tables 1-5 summarize the simulation model parameters. The PV inverters are the SMA Sunny Central HE series (SMA500HE and SMA630HE). These inverters are voltage source inverters (VSI) and are classified as high-frequency, pulse-width modulated current-regulated inverters. A STATCOM (GPCOM model) of 2 MVar is added at node 91. When capacitor banks are used, they are connected at bus 100.

Node	Name	Voltage [kV]
1	XFMR.STAT.1	20
2	XFMR.STAT.2	20
3	XFMR.STAT.3	20
4	XFMR.STAT.4	20
5	XFMR.STAT.5	20
6	XFMR.STAT.6	20
7	XFMR.STAT.7	20
8	XFMR.STAT.8	20
11	SMA500HE.01	0.270
12	SMA500HE.02	0.270
21	SMA630HE.03	0.315
22	SMA630HE.04	0.315
31	SMA630HE.05	0.315
32	SMA630HE.06	0.315
41	SMA630HE.07	0.315
42	SMA630HE.08	0.315
51	SMA630HE.09	0.315
61	SMA500HE.10	0.270
62	SMA500HE.11	0.270
71	SMA630HE.12	0.315
72	SMA630HE.13	0.315
81	SMA500HE.15	0.270
82	SMA500HE.16	0.270
91	GPCOM	0.700
100	OUT.PV.PCC	20
101	CEZ.POI	20
102	VANJ.MAR.POI	110
301	BANOVITA	110
501	MV.XFMR.09	20
502	MV.XFMR.10	20
503	HV.XFMR.09	110
504	HV.XFMR.10	110

Table 1: Grid nodes

Node	Name	Voltage [kV]	Short circuit power [MVA]	Short circuit ratio (X/R)
102	Vanj.MAR.POI	110	1000	10

Table 2: Equivalent grid data

Node 1	Node 2	V_p [kV]	V_s [kV]	S_{nom} [MVA]	r [p.u]	x [p.u]
503	501	110	20	16	0.0	0.676
504	502	110	20	10 (out of service)	0.0	0.112
100	91	20	0.69	2	0.0	0.06
5	51	20	0.315	0.63	0.0114	0.0589

Table 3: 2 winding transformer data

Node 1	Node 2	Node 3	V_p [kV]	V_s [kV]	V_t [kV]	S_{nom} [MVA]	r + jx [p.u]
1	11	12	20	0.27	0.27	1 (Primary) 0.5 (secondary) 0.5 (tertiary)	0.0053+j0.0592 (p-s) 0.0059+j0.0597 (p-t) 0.0055+j0.0592 (s-t)
2	21	22	20	0.315	0.315	1.26 (Primary) 0.63 (secondary) 0.63 (tertiary)	0.0050+j0.0598 (p-s) 0.0042+j0.0599 (p-t) 0.0051+j0.0598 (s-t)
3	31	32	20	0.315	0.315	1.26 (Primary) 0.63 (secondary) 0.63 (tertiary)	0.0050+j0.0598 (p-s) 0.0042+j0.0599 (p-t) 0.0051+j0.0598 (s-t)
4	41	42	20	0.315	0.315	1.26 (Primary) 0.63 (secondary) 0.63 (tertiary)	0.0050+j0.0598 (p-s) 0.0042+j0.0599 (p-t) 0.0051+j0.0598 (s-t)
6	61	62	20	0.27	0.27	1 (Primary) 0.5 (secondary) 0.5 (tertiary)	0.0053+j0.0592 (p-s) 0.0059+j0.0597 (p-t) 0.0055+j0.0592 (s-t)
7	71	72	20	0.315	0.315	1.26 (Primary) 0.63 (secondary) 0.63 (tertiary)	0.0050+j0.0598 (p-s) 0.0042+j0.0599 (p-t) 0.0051+j0.0598 (s-t)
8	81	82	20	0.27	0.27	1 (Primary) 0.5 (secondary) 0.5 (tertiary)	0.0053+j0.0592 (p-s) 0.0059+j0.0597 (p-t) 0.0055+j0.0592 (s-t)

Table 4: 3 winding transformer data

Node 1	Node 2	Line R [Ω]	Line X [Ω]	Line C [μF]
1	2	0.0244	0.0201	0.0597
2	3	0.0863	0.0107	0.2111
3	4	0.0293	0.0241	0.0716
4	6	0.0494	0.0407	0.1209
5	6	0.0244	0.0201	0.0597
5	7	0.0731	0.0603	0.0179
7	8	0.0540	0.0445	0.1322
1	100	0.0423	0.0348	0.1034
8	100	0.1313	0.1082	0.3213
100	101	0.3605	0.2013	1.771
102	301	0.0000	0.0121	0.0000

Table 5: Line data

(a) Vanju-Mare PV plant image [27]

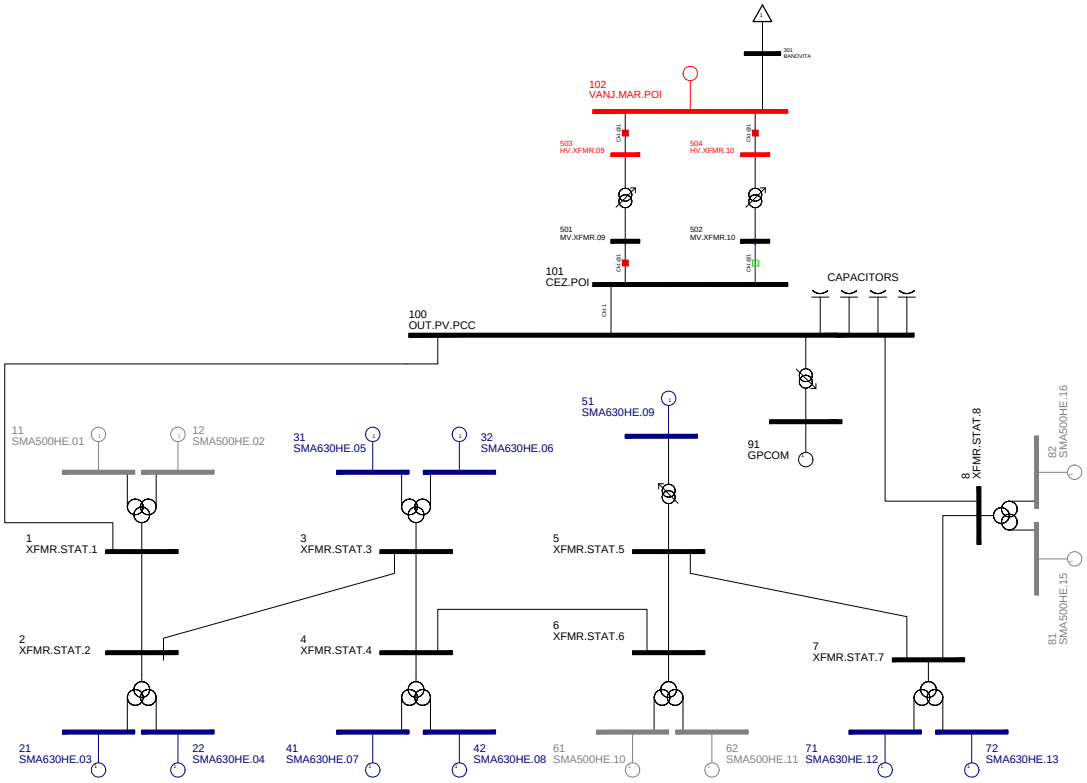

(b) Scheme of Vanju-Mare simulation model in PSS/E®. Red = 100 kV, black = 20 kV, blue = 0.315 kV, grey = 0.27 kV

Fig. 5: Vanju-Mare PV plant

3.2 Simulation Results

All the simulation results are obtained in PSS/E®.

Figure 6 shows the response at PCC after setting active and reactive power setpoints and a power factor setpoint (simulation 1). This is performed in a PV plant only equipped with inverters. In Figure 6(a), it is shown the active and reactive power response, the corresponding setpoints and the ramp limitation. At Figure 6(b), it is shown the power factor response as well as the power factor control flag (the activation signal of power the factor control mode). It can be observed a power curtailment at the beginning and how the ramp limiter, as well as the measured active power, respond properly. At second 80 of the simulation, the reactive power setpoint is changed. The results show again a good response and in addition, the capacity to perform independent active and reactive power controls. At second 250, the power factor flag is set and the corresponding setpoint is stepped-down to 0.90. As a

result, in the upper plot it can be observed that the reactive power setpoint is recalculated to obtain the desired power factor. At second 350, a power curtailment is set and, as the power factor control remains active, the reactive power setpoint recalculation to maintain the power factor at 0.90 is observed. These results can be concluded as appropriate for curtailment and reactive setpoint events as well as for the power factor control mode.

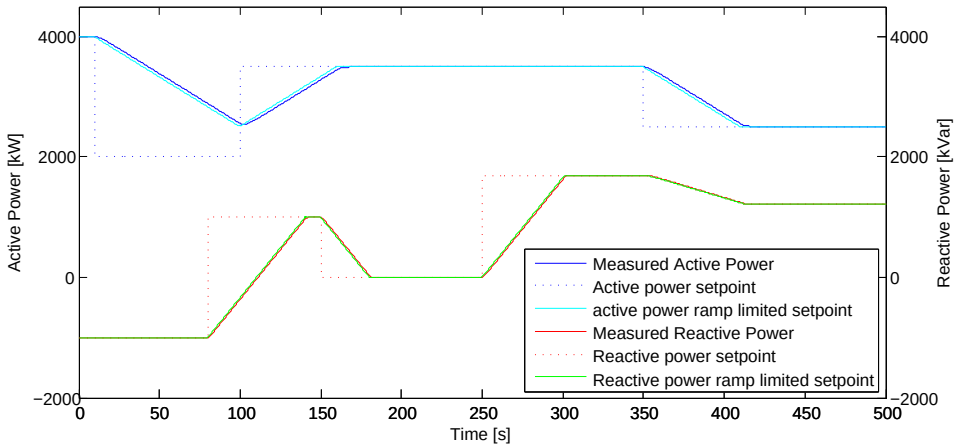

(a) Active and reactive power

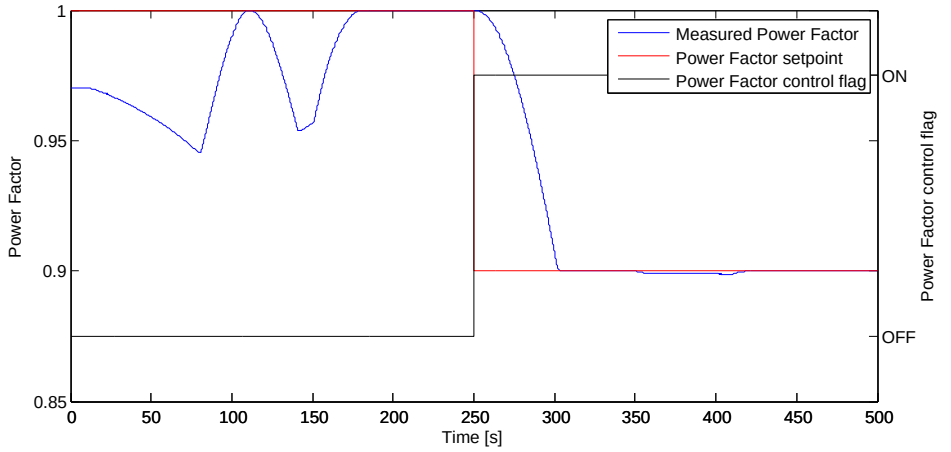

(b) Power factor

Fig. 6: Control response of: active power, reactive power and power factor setpoints (simulation 1)

In Figure 7(a), the frequency droop operation can be observed (simulation 2). In this case, the simulation begins with an active power setpoint with ramp limitation. The frequency droop control flag is set at second 200 of the simulation. In this case, the droop curve is defined by: $P_{TSO} = P_{available} = 4$ MW, $f_n = 50$ Hz, $f_3 = 50.5$ Hz, $f_4 = 52$ Hz, $f_{max} = 53$ Hz, $P_{max} = 4$ MW and $P_{min} = 1$ MW. Furthermore, the active power contribution from droop control is not limited by a ramp rate. To perform the simulation, the frequency is not measured but set manually to test the different droop curve zones. First, it can be observed when the frequency is in the deadband range, that the active power setpoint doesn't change. Once it is over the deadband (51 and 52.0 Hz), the active power setpoints changes according to the droop curve and the real power achieves these new levels. Between f_4 and f_{max} the active power setpoint remains constant at P_{min} as it can be seen in the last frequency step. The result shows an appropriate behaviour of the frequency droop control.

Figures 7(b) and 7(c) show the voltage droop control mode response (simulation 3). In the simulation case, 4 capacitor banks of 500 kVar have been added. Figure 7(b) shows the reactive power setpoint, Q^* in red, the measured reactive power in blue and the measured voltage in green. The ramp rate limiter is deactivated when the voltage droop operation is set (as usually required by TSO). At the beginning a reactive power setpoint mode sets a down-step setpoint and the ramp limiter is active. It can be observed how the capacitor banks disconnect when Q^* decreases enough, followed by the corresponding correction by PV inverters (Figure 7(c)). Then, at ond 100, the voltage droop control mode is set. The droop curve is defined by a deadband between 0.98 and 1.02 p.u, $Q_{max} = 6.2$ MVar, $Q_{min} = -4.2$ MVar and $K_{droop} = 5\%$ where K_{droop} is the slope of the droop curve. It can be observed the first voltage step (0.99 p.u) is inside the deadband and so, the reactive power setpoint is not modified. Then, the

voltage decreases by steps (0.96, 0.94, 0.9, 0.85 and 0.75 p.u respectively). The corresponding reactive power setpoint according to the droop curve can be observed. When the grid voltage changes to 0.96 p.u, the reactive power setpoint is 2.48 MVar, so, all capacitor banks are connected and the remaining reactive power is delivered by the inverters (bottom plot). Then, as the voltage decreases, inverters deliver the additional required reactive power as all capacitors are connected.

Finally, the filter response performance is shown in Figure 8 (simulation 4). In this case 6 capacitor banks and a STATCOM of 2 MVar have been added. The operation mode is the voltage droop and in second 2, the grid voltage steps down. Therefore, reactive power needs to be injected. Figure 8(a) shows the reactive power injected at PCC in 3 scenarios: without filter (green line), with a filter time constant of 0.15 s (red line) and with filter time constant of 0.5 s (blue line). Figure 8(b) depicts the voltage measured at PCC (solid lines) and the corresponding filter outputs (dashed lines) and finally, the capacitor banks connections are shown in Figure 8(c). As it can be observed, when there isn't any filter, the connection of a capacitor bank provokes an increase of voltage. As a result, the reactive power required steps down and the capacitor bank disconnects. It happens successively provoking multiple connections and disconnections. To avoid this phenomenon, a filter is set at the voltage measurement, avoiding fast changes. It can be observed that the slower the filter, the more stable is the response. In this case, a filter with time constant of 0.5 s was enough to obtain a stable operation.

All the PV inverters are the same type (SMA Sunny Central HE) with the same response time. In case of different types of inverters installed, the PI of the power plant controller will correct the P_{tot} and Q_{tot}. The steady state values of the PI output will be the same, but the transient behaviour can be different. The reason being, some inverters will reach the active and reactive power setpoints before others, so the input of the PI controller of the PPC will change showing a different transient than if all the inverters were the same. In fact, in the case of having a sampling time of the PPC slower than the response time of the slowest inverter, the same transient behaviour should be observed.

4 Power Plant Control Implementation and Results

4.1 Implementation

The power plant control has been implemented as shown in Figure 9. The main elements of the whole PPC system are the GPM PV SCADA, the GPM PPC controller, the GPM Smart Bridge and the communication system.

Each RTU system is associated with a set of inverters, FACTS devices, batteries, capacitor banks or to the point of interconnection (POI) meter. RTUs allow the sending/receiving of data to/from any PV inverter or other elements.

The PV SCADA will collect and display on a screen all PV plant information in real time. It will also allow the user to set the control mode and the local setpoints ($P^*_{pre-ramp}$, $Q^*_{pre-ramp}$, etc.). As the PV SCADA system is thought only to display and interact with the PV power plant, another system is still required to implement the PPC and hence, the PV SCADA needs to send the control mode and setpoints to this system.

The Smart Bridge receives data from PV SCADA and from the TSO, interacts with the PPC controller and sends the PPC orders to all inverters, capacitor banks or other elements.

The Power Plant Controller receives the setpoints coming from the PV SCADA or from the TSO through the Smart Bridge. It also receives measurements directly from PCC (in order to avoid delays through the Smart Bridge) and executes the control algorithm explained previously. The algorithm outputs are sent from the PPC controller to all inverters or any other element through the Smart Bridge system.

4.2 Results

The following results correspond to a 9.4 MW PV power plant in Romania (Vanju-Mare PV plant). After the PPC implementation, a set of tests were carried out to verify that the PV plant behaviour was correct. The tests were performed from 10h 45min until 13h 11min on a cloudy day and the data results were obtained every 500ms. Due to the fact that capacitor banks were not installed in the PV plant, the PPC actions regarding these elements could not be tested in a real application.

Figure 10(a) depicts the active power measured and the corresponding setpoint at PCC. It can be observed that 3 curtailments have been tested. In this PV plant, PV inverters responses are extremely slow (time constant of about 10 seconds). So, in the first curtailment attempt the sampling time has been set to 10 seconds; time enough to achieve the P^* setpoint before sending a new setpoint. This way, some steps in the ramp response can be observed. At the end of the first curtailment, the available active power decreased, so the following ramp-up response could not be observed. In the second curtailment, an attempt to reduce the stepping during the ramp event has been done. The sampling time has been set faster than the PV inverter dynamics (1 second). This way, a ramp event improvement could be observed. Furthermore, after the second curtailment, the ramp-up event is performed perfectly as the available active power was high enough. The third curtailment confirms the appropiate control response.

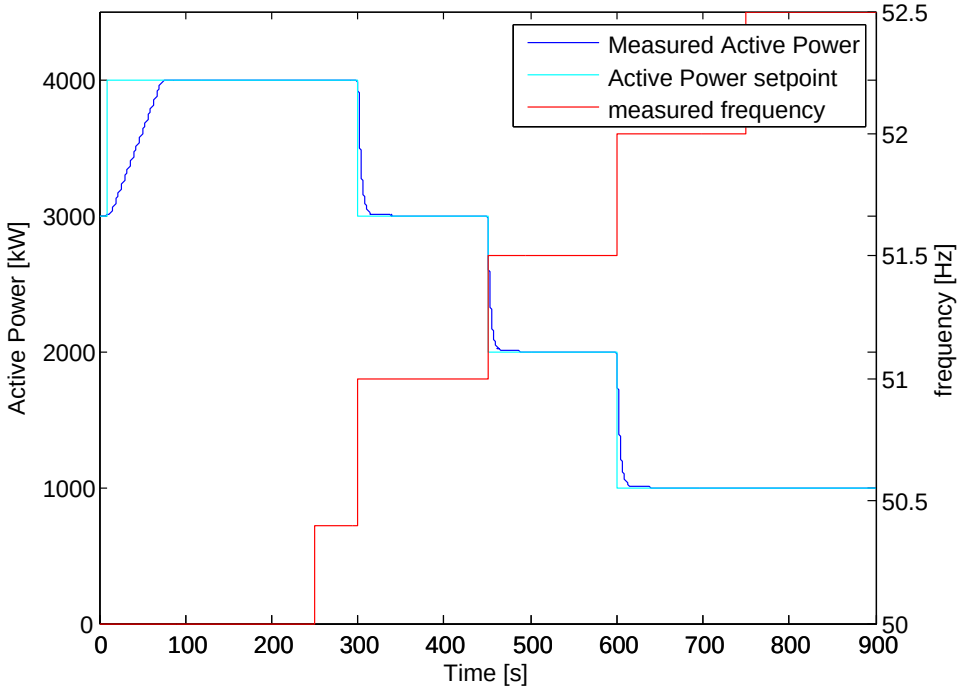

(a) Frequency droop response (simulation 2)

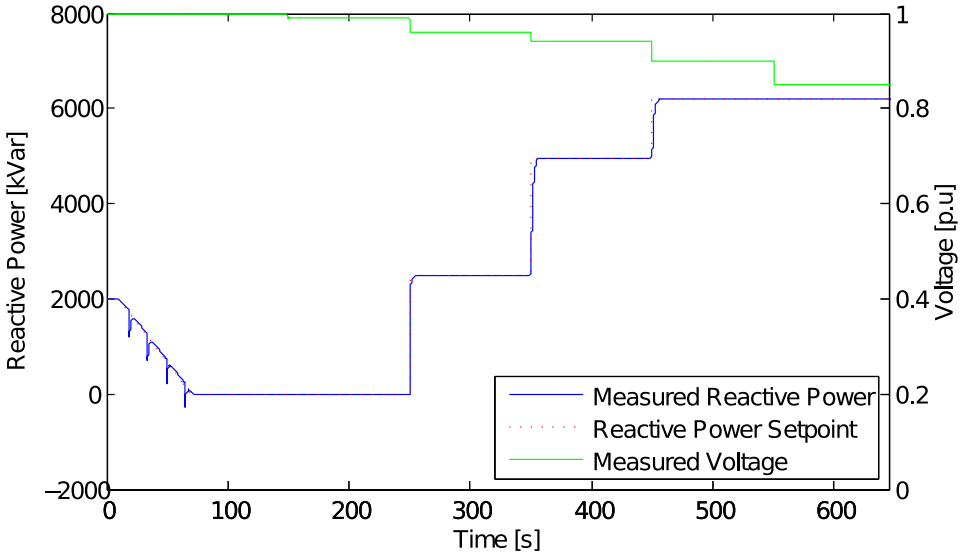

(b) Voltage droop response (simulation 3)

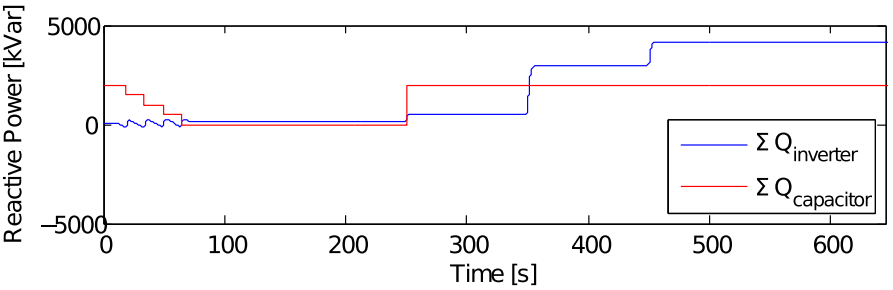

(c) Inverter and capacitor banks reactive power injection during voltage droop operation (simulation 3)

Fig. 7: Control droop modes response (simulations 2 and 3)

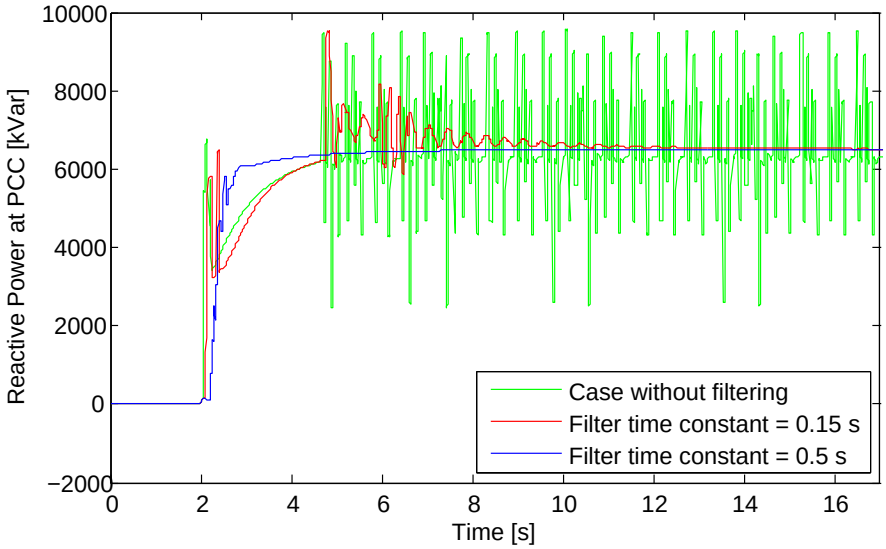

(a) Reactive power at PCC

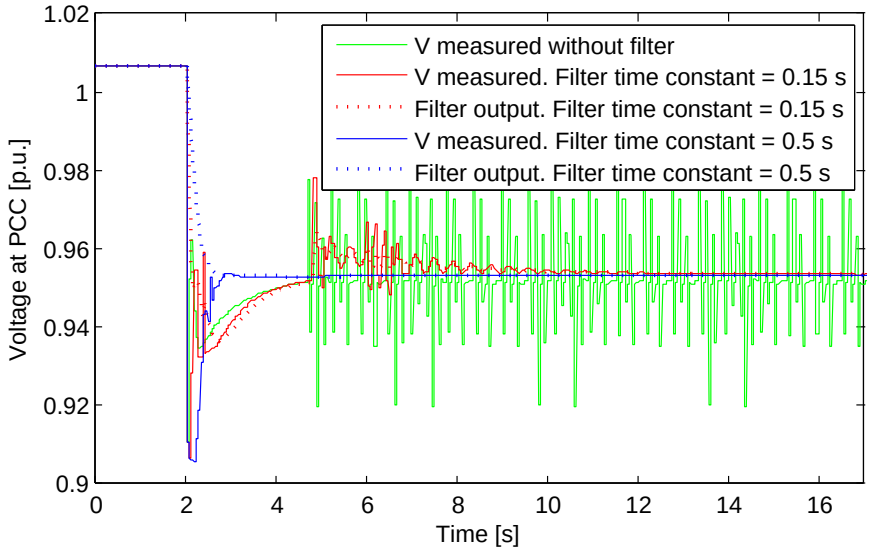

(b) Voltage at PCC

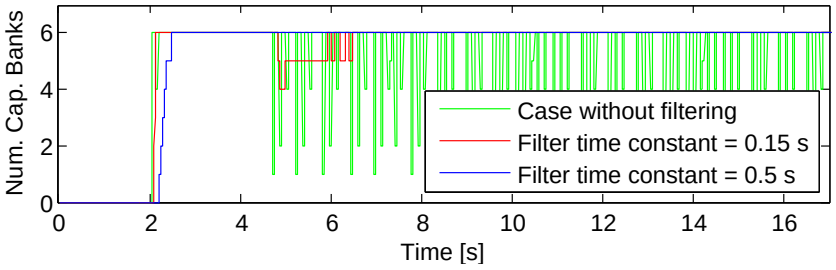

(c) Capacitor banks connections and disconnections

Fig. 8: Filter response performance (simulation 4)

Reactive power response has also been studied. Figure 10(b) depicts the reactive power measurement and its corresponding setpoint at PCC during the tests. At the beginning β and γ are set directly to 0. So, the reactive power measured is the one generated by transformers and cables. After the first reactive power setpoint these values become controlled (the variations around second 3000 and after second 8000 are due power factor control tests). Analysing the reactive power setpoints and the response behaviour (in this case, a reactive ramp rate limiter was requested by the TSO) it can be concluded that the reactive power control fulfils the grid code.

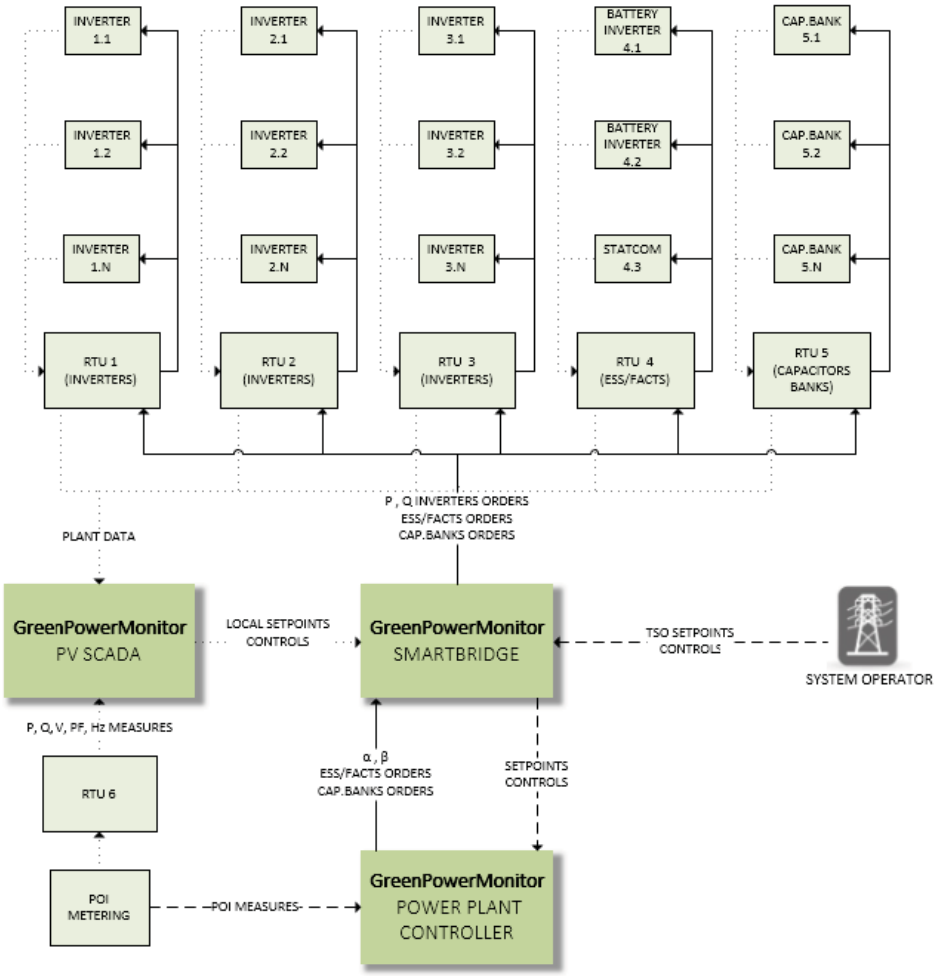

Fig. 9: PPC implementation scheme

Power factor control response is shown in the upper plot of Figure 11(a). Until the second 8147, the power factor control is disabled but reactive power setpoint is set to 0. Then, a 0.97 setpoint is applied. In Figure 11(b), it can be observed how the reactive power setpoint is changed automatically according to (2). Due to the low active power variability at the beginning, the reactive power setpoint is nearly constant. Then, a power curtailment is performed 11(c) and the reactive power setpoint reacts to it to maintain the power factor.

In general, the real results presented show a good performance of the PV plant with the explained PPC. Other control results, such as voltage or frequency droop, are based on calculating the necessary active or reactive power setpoints (it has been proven they work under simulation tests) and none of them has presented any grid code breach from its start up until now (8 months).

As a final and more general result, the presented PPC has been implemented in other PV plants in Romania (all about 10 MW), in a South African PV plant (more than 60 MW), and two large scale PV plants in the U.S. are at the end stage of the PPC implementation process. In all cases, the fulfilment of the corresponding grid code is achieved.

5 Conclusion

In this paper, the different stages for designing and implementing a PV power plant controller according to the author's experience have been presented. The control algorithm has been designed for a generic PV power plant, where its robustness has permitted it to be implemented in several PV plants (with different devices installed) and to accomplish different grid codes.

The power plant control proposed has covered a general and complete approach. In addition, taking into consideration typical ancillary devices for voltage support actions (FACTS and capacitor banks), a new dispatching system based on priorities has been implemented satisfactorily. This dispatching system is designed to be flexible in order to be adapted to any PV power plant provided with FACTS, capacitor banks, both ancillary devices or none of them.

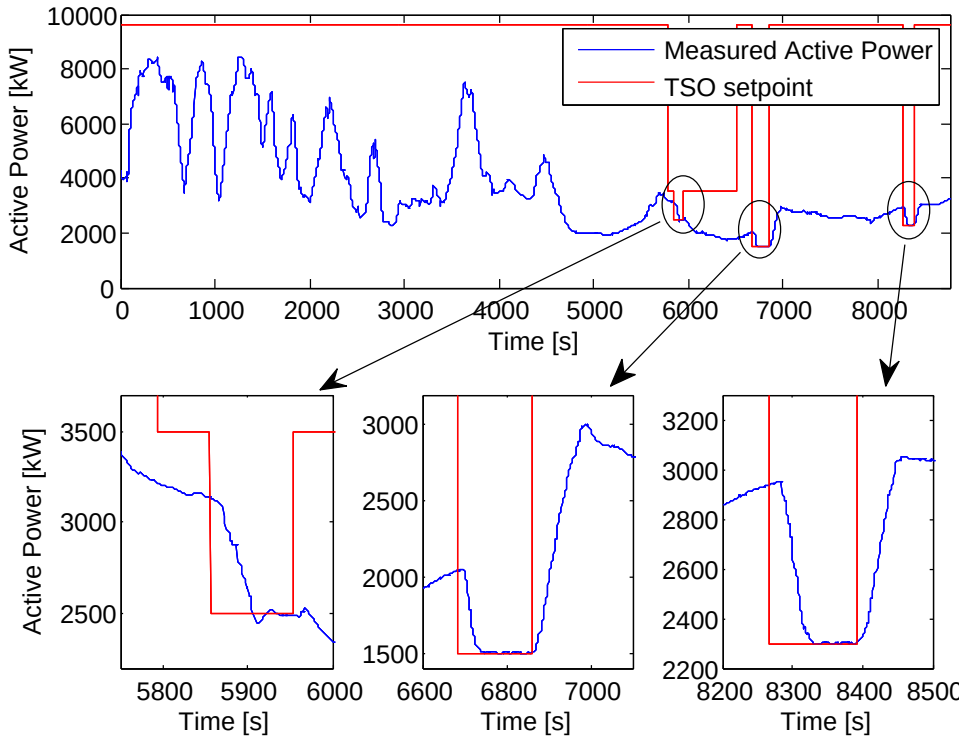

(a) Active power response

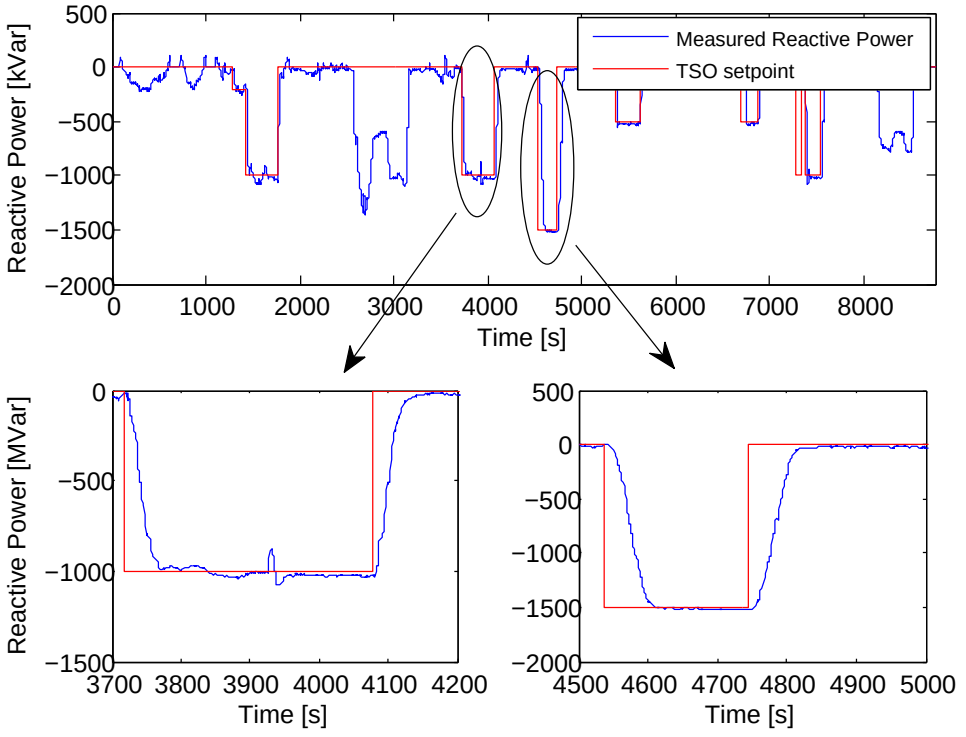

(b) Reactive power response

Fig. 10: Active and reactive power response in Vanju-Mare PV plant

A generic PSS/E® (and DIgSILENT Power Factory®) power plant controller model has been created to be used by system operators or other users. It should allow them to perform their own studies. Some simulation results have been presented showing its appropriate behaviour.

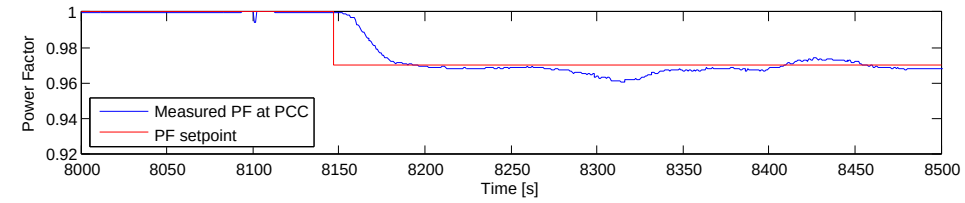

(a) Power factor

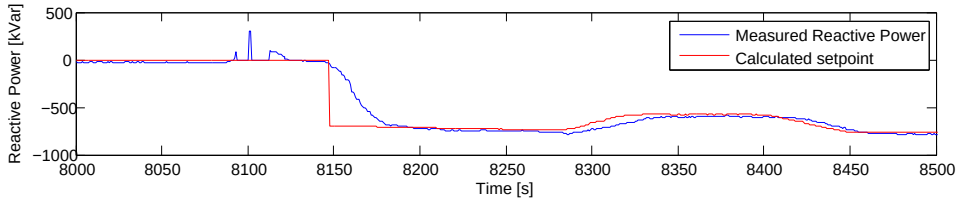

(b) Reactive power

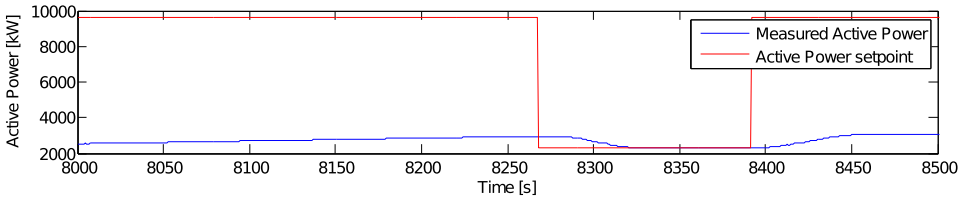

(c) Active power

Fig. 11: Power Factor response in Vanju-Mare PV plant

Finally, after monitoring a 9.4 MW Romanian PV plant, real results have been presented.

Acknowledgements

The authors would like to thank EDPR for providing the PV plant data, which have been utilized in the simulation models as well as for giving permission to publish the results obtained in its real PV plant and Marta Massagué for proofreading this paper. This work has been funded by the Spanish Ministry of Economy and Competitiveness under the projects ENE2012-33043 and ENE2013-47296. This research was co-financed by the European Regional Development Fund (ERDF). The research leading to these results has received support of the Secretaria d'Universitats i Recerca del Departament d'Economia i Coneixement de la Generalitat de Catalunya and has been co-funded by the European Social Fund. The research leading to these results has received funding from the European Union Seventh Framework Program FP7-ICT-2013-11 under grant agreement 619610 (Smart Rural Grid).

References

[1] European Commission. *Communication from the commission to the European Council and the European Parliament - An energy policy for Europe*. Commission of the European Communities, 2007.

[2] *Medium-Term Market Report Executive Summary 2014. Market Analysis and Forecasts to 2020.* IEA, International Energy Agency.

[3] Rabia Ferroukhi et al. *REthinking Energy, 2014*. IRENA, International Renewable Energy Agency, 2014.

[4] Jacopo Moccia Ivan Pineda, Sarah Azau and Justin Wilkes. *Wind in power. 2013 European statistics*. EWEA, European Wind Energy Association, 2014.

[5] Berndt et al. *Transmission code 2007 - Network and system rules of the German transmission system operators*. Verband der Netzbetreiber - VDN - e.V. beim VDEW, 2007.

[6] *Grid connection code for renewable power plants (RPPs) connected to the electricity transmission system (TS) or the distribution system (DS) in South Africa*. 2012.

[7] *Technical transmission grid code of the Romanian power system*. Romanian Power Grid Company TRANSELECTRICA S.A., 2004.

[8] *Minimum technical requirements for interconnection of photovoltaic (PV) facilities*. Puerto Rico Electric Power Authority. PREPA, 2012.

[9] Ben Noone. *PV integration on Australian distribution networks. Literature review*. The Australian PV Association, 2013.

[10] *Standard large generator interconnection agreement (LGIA) among interconnection customer and California Independent system operator corporation*.

[11] S. Teleke, M.E. Baran, S. Bhattacharya, and A.Q. Huang. Rule-based control of battery energy storage for dispatching intermittent renewable sources. *IEEE Transactions on Sustainable Energy*, 1(3):117–124, Oct 2010.

[12] H. Gaztanaga, J. Landaluze, I. Etxeberria-Otadui, A. Padros, I. Berazaluce, and D. Cuesta. Enhanced experimental pv plant grid-integration with a mw lithium-ion energy storage system. In *2013 IEEE Energy Conversion Congress and Exposition (ECCE)*, pages 1324–1329, Sept 2013.

[13] R. van Haaren, M. Morjaria, and V. Fthenakis. Utility scale pv plant variability and energy storage for ramp rate control. In *2013 IEEE 39th Photovoltaic Specialists Conference (PVSC)*, pages 0973–0979, June 2013.

[14] M.J.E. Alam, K.M. Muttaqi, and D. Sutanto. A novel approach for ramp-rate control of solar pv using energy storage to mitigate output fluctuations caused by cloud passing. *IEEE Transactions on Energy Conversion*, 29(2):507–518, June 2014.

[15] Guishi Wang, M. Ciobotaru, and V.G. Agelidis. Power smoothing of large solar pv plant using hybrid energy storage. *IEEE Transactions on Sustainable Energy*, 5(3):834–842, July 2014.

[16] Weidong Xiao, K. Torchyan, M.S. El Moursi, and J.L. Kirtley. Online supervisory voltage control for grid interface of utility-level pv plants. *IEEE Transactions on Sustainable Energy*, 5(3):843–853, July 2014.

[17] E. Bullich-Massagué, M. Aragüés-Peñalba, R. Ferrer-San-José, L. Serrano-Salamanca, C. Pacheco-Navas, and O. Gomis-Bellmunt. Power plant control experience in large scale pv plant. Modelling, control, simulation and implementation. In *4th International Workshop on Integration of Solar into Power Systems, Berlin*, November 2014.

[18] Jorge Martínez, Pedro Rodriguez, Philip C. Kjær, and Remus Teodorescu. Design and coordination of a capacitor and on-load tap changer system for voltage control in a wind power plant of doubly fed induction generator wind-turbines. *Wind Energy*, 15(4):507–523, 2012.

[19] Jaesung Jung, Ahmet Onen, Reza Arghandeh, and Robert P. Broadwater. Coordinated control of automated devices and photovoltaic generators for voltage rise mitigation in power distribution circuits. *Renewable Energy*, 66(0):532 – 540, 2014.

[20] R.K. Varma, S. Rahman, and T. Vanderheide. New control of pv solar farm as statcom (pv-statcom) for increasing grid power transmission limits during night and day. *IEEE Transactions on Power Delivery*, PP(99):1–1, 2014.

[21] Liu Yaoyuan, Zeng Chengbi, Miao Hong, and Fu Wenwen. Research on a new method to achieve low voltage ride through of pv. In *2014 International Conference on Power System Technology (POWERCON)*, pages 1064–1070, Oct 2014.

[22] *IEA PVPS Task 8: Project Proposals on Very Large Scale Photovoltaic Power Generation (VLS-PV) Systems in Deserts*, volume 2. May 2006.

[23] M. Datta, T. Senjyu, A. Yona, T. Funabashi, and Chul-Hwan Kim. A coordinated control method for leveling pv output power fluctuations of pv-diesel hybrid systems connected to isolated power utility. *Energy Conversion, IEEE Transactions on*, 24(1):153–162, March 2009.

[24] Xing Luo, Jihong Wang, Mark Dooner, and Jonathan Clarke. Overview of current development in electrical energy storage technologies and the application potential in power system operation. *Applied Energy*, 137:511 – 536, 2015.

[25] Ehs annual monitoring report. 2012.

[26] http://en.grupotsk.com/proyectos/vanju-mare [accessed in january 2015].

[27] http://www.schrack-seconet.com [accessed in january 2015].